The Allee Effect and Infectious Diseases: Extinction, Multistability, and the (Dis-)Appearance of Oscillations

Frank M. Hilker,[1,*] Michel Langlais,[2,†] and Horst Malchow[3,‡]

1. Center for Mathematical Biology, Mathematical and Statistical Sciences, University of Alberta, 501 CAB, Edmonton, Alberta T6G 2G1, Canada;
2. Université Victor Segalen Bordeaux 2, Institut de Mathématiques de Bordeaux Unité Mixte de Recherche Centre National de la Recherche Scientifique 5251 and Institut National de Recherche en Informatique et en Automatique Bordeaux Sud-ouest projet Anubis, case 26, Unité de Formation et de Recherche Sciences et Modelisation, 146, rue Leo Saignat, 33076 Bordeaux Cedex, France;
3. Institute for Environmental Systems Research, Department of Mathematics and Computer Science, University of Osnabrück, 49069 Osnabrück, Germany

Submitted September 25, 2007; Accepted July 15, 2008; Electronically published December 5, 2008

abstract: Infectious diseases that affect their host on a long timescale can regulate the host population dynamics. Here we show that a strong Allee effect can lead to complex dynamics in simple epidemic models. Generally, the Allee effect renders a population bistable, but we also identify conditions for tri- or monostability. Moreover, the disease can destabilize endemic equilibria and induce sustained oscillations. These disappear again for high transmissibilities, with eventually vanishing host population. Disease-induced extinction is thus possible for density-dependent transmission and without any alternative reservoirs. The overall complexity suggests that the system is very sensitive to perturbations and control methods, even in parameter regions with a basic reproductive ratio far beyond $R_0 = 1$. This may have profound implications for biological conservation as well as pest management. We identify important threshold quantities and attribute the dynamical behavior to the joint interplay of a strong Allee effect and infection.

* Corresponding author. Present address: Centro de Matemática e Aplicações Fundamentais, Universidade de Lisboa, Complexo Interdisciplinar–Avenida Prof. Gama Pinto 2, 1649-003 Lisboa, Portugal; e-mail: fhilker@ptmat.fc.ul.pt.

† E-mail: langlais@sm.u-bordeaux2.fr.

‡ E-mail: malchow@uos.de.

Am. Nat. 2009. Vol. 173, pp. 72–88. 0003-0147/2009/17301-50360$15.00.
DOI: 10.1086/593357

Keywords: epidemiology, Allee effect, SI model, periodic oscillation, multistability, disease-induced extinction.

Introduction

Infectious diseases and parasites can be important drivers of their host population (Anderson and May 1979; Hudson et al. 2001) and are held responsible for a large number of extinctions (Daszak et al. 1999; Harvell et al. 2002; Smith et al. 2006). While mathematical models have greatly contributed to the understanding of disease dynamics (Bailey 1975; Anderson and May 1991; Diekmann and Heesterbeek 2000), the vast majority of models are based on only simple demographic processes. This is probably due to a prevailing interest in human epidemics, in which the timescale of the disease is short and host demography can thus often be ignored. Many animal populations, however, are affected by fatal diseases on a timescale that is not negligible in comparison with the life expectancy. Here we show that the existence of a strong Allee effect (population decline at small densities) can lead to surprisingly rich dynamics in a basic epidemiological model, including sustained oscillations, multiple steady states, and catastrophic collapses of endemic equilibria.

Disease is becoming increasingly recognized as a major factor in conservation biology and population viability analysis (Haydon et al. 2002; Lafferty and Gerber 2002; Gerber et al. 2005). The Serengeti disease outbreaks of rabies and canine distemper virus in wild carnivore populations over the past 20 years raised the awareness that pathogens are of acute importance for small and endangered species (Cleaveland et al. 2007). The impact of disease can be particularly devastating in populations with a strong Allee effect, since any further reduction might tip the population density below the critical threshold and lead to extinction. Examples of species that suffer from both disease and an Allee effect include the African wild dog *Lycaon pictus* (Burrows et al. 1995; Courchamp et al. 2000) and the island fox *Urocyon littoralis* (Clifford et al. 2006; Angulo et al. 2007). Allee effects can be caused by a number of mechanisms, for instance, difficulties in find-

ing mating partners at low population densities and inbreeding (e.g., Allee 1938; Courchamp et al. 1999; Stephens and Sutherland 1999; Stephens et al. 1999). It has also been hypothesized that animal species that aggregate as a consequence of the Allee effect (e.g., for social thermoregulation, antipredator vigilance, or predator dilution) would be more prone to parasitism (Christe et al. 2006, p. 599), since there is a positive relationship between host social behavior and parasite prevalence, intensity (number of parasites within a host), and diversity (e.g., Møller et al. 1993; Altizer et al. 2003).

Although small populations are the most commonly cited reason for disease-induced extinctions (de Castro and Bolker 2005), the joint interplay of infection and Allee effects has been addressed only recently in theoretical models (partially also taking into account spatiotemporal dynamics; see Hilker et al. 2005; Petrovskii et al. 2005). Dobson and Poole (1998) do not explicitly incorporate an Allee effect in the host population but modify the disease transmission function to show that spatial aggregation increases the likelihood of infection. Deredec and Courchamp (2006) and Hilker et al. (2007) demonstrate that disease mortality increases the minimum viable population density, below which the host becomes extinct. In a previous model with frequency-dependent transmission, the latter authors find analytical conditions that lead to two endemic states, one of which is always unstable, while the other one is always stable. There also is a disease-induced extinction state, in which the parasite drives the host population to extinction and which can be the only stable equilibrium, thus breaking the bistability inherent in strong Allee dynamics. Deredec and Courchamp (2006) report that the host size depression due to disease is larger in a model with Allee effect rather than with logistic population growth. Furthermore, populations with Allee effect are better protected against parasite invasion. They claim that their analysis is "mostly applicable" (Deredec and Courchamp 2006, p. 676) to a number of models considering both frequency- and density-dependent transmission. In this article, however, we show that more complicated dynamical regimes are possible if transmission is density dependent.

The organization of this article is as follows. First, we describe the mathematical model and its underlying assumptions. Although we have mostly epizootiological problems in mind, we will use epidemiological terminology throughout this article because the model is very general. It may be applied to infectious diseases and hosts with similar characteristics. We then introduce several threshold quantities, among them the basic and effective reproductive ratio as well as the disease threshold (critical host density for disease establishment). These allow us to categorize the number of endemic (nontrivial) equilibria. We also give conditions for the stability of the (semi-)trivial—that is, disease-free—equilibria. Next, we present numerical bifurcation analyses. These reveal the stability properties of the endemic equilibria and the appearance as well as disappearance of periodic solutions. We illustrate our findings in numerical simulations with parameter values, for which the circulation of the feline immunodeficiency virus within populations of domestic cats (*Felis catus*) may be seen as an example. The following section is devoted to an overview of the system dynamics in a two-parameter diagram. It turns out that the dynamical behavior can be summarized mathematically by a Bogdanov-Takens point. Finally, we provide conclusions of our findings and discusses their potential limitations and impacts.

Model Description and Assumptions

Model Structure

Let $N = N(T) \geq 0$ denote the host population density at time $T \geq 0$. In the presence of an infectious disease, the total population $N = X + Y$ is split into a susceptible (X) and an infected (Y) part. We assume that there is no recovery from disease. The transfer diagram of the model considered is as follows:

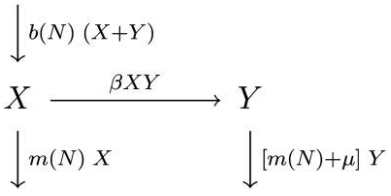

The transmission is assumed to be density dependent and described by the mass action rate βXY, with coefficient $\beta > 0$ (see McCallum et al. 2001). There is no vertical transmission; that is, infecteds do not transmit the disease to their offspring. Hence, infecteds reproduce into the susceptible class, and the per capita net growth function is split into $g(N) = b(N) - m(N)$, with $b(N) \geq 0$ being the fertility function and $m(N) \geq 0$ being the natural mortality function. Infecteds suffer an additional disease-related mortality, which is described by the virulence $\mu > 0$. The model equations read

$$\frac{dX}{dT} = -\beta XY + b(N)N - m(N)X,$$

$$\frac{dY}{dT} = \beta XY - m(N)Y - \mu Y.$$

We now specify the demographic functions and assume

that a strong Allee effect is manifested by the following per capita net growth rate:

$$g(N) = a(K_+ - N)(N - K_-), \tag{1}$$

with K_+ being the carrying capacity, K_- being the minimum viable density of the disease-free population (Allee threshold), and $0 < K_- \ll K_+$ in most cases of ecological interest. The parameter $a > 0$ adjusts the maximum per capita growth rate; compare this with similar functional forms in the studies of Lewis and Kareiva (1993), Gruntfest et al. (1997), Amarasekare (1998), and Courchamp et al. (1999). Function (1) can be obtained by assuming a density-dependent per capita mortality rate (analogously to logistic growth) and a quadratic per capita fertility rate:

$$b(N) = a[-N^2 + (K_+ + K_- + e)N + c], \tag{2}$$

$$m(N) = a(eN + K_+K_- + c). \tag{3}$$

Qualitatively similar fertility rates have been used by Hopf and Hopf (1985) and Wang et al. (1999). They can be traced back to Volterra (1938); see also Dennis (1989). The present choice of demographic functions describes populations with linearly increasing mortality, mate encounters based on bimolecular collisions (i.e., the number of meetings between the two sexes is proportional to N^2), and a linearly decreasing offspring survival in crowded habitats (see Boukal and Berec 2002). In order to guarantee $b(N)$ to be positive, we restrict our attention to the case $N \leq K_+ + K_- + e$, which is sufficient for our model because any initial population density below or close to the carrying capacity will be bounded from above by K_+. Parameters e, $c \geq 0$ determine the effect of density dependence and independence in the demographic functions, respectively. They do not affect the intrinsic per capita growth rate $g(N)$.

Introducing the dimensionless quantities

$$P = \frac{N}{K_+},\ I = \frac{Y}{K_+},\ t = aeK_+T > 0,$$

$$r = \frac{K_+}{e} > 0,\ u = \frac{K_-}{K_+} \in (0, 1),\ d = \frac{c}{eK_+} > 0,$$

$$\sigma = \frac{\beta}{ae} > 0,\ \alpha = \frac{\mu}{aeK_+} \geq 0,$$

we can write our model as

$$\frac{dP}{dt} = r(1 - P)(P - u)P - \alpha I, \tag{4}$$

$$\frac{dI}{dt} = [-\alpha - d - ru + (\sigma - 1)P - \sigma I]I \tag{5}$$

in the (P, I) phase plane. Parameter P is the dimensionless total population that is composed of infecteds (I) and susceptibles ($P - I$). Note the convenient notation of the cubic growth term for the total population in equation (4). In the rest of this study, we shall focus on the ecologically interesting case in which the Allee threshold is far from the carrying capacity, $0 < u < 1/2$.

Exemplary Application: FIV in Domestic Cats

In order to illustrate the dynamics of model (4)–(5), we will later employ parameter values taken from studies of the feline immunodeficiency virus (FIV) circulating within populations of domestic cats. Here we briefly describe this system's ecology and epidemiology. Although we are not aware of any article addressing potential Allee effects in cat populations, the domestic cat appears to be an interesting study subject because of the great variety in its spatial organization and social behavior. These are believed to depend primarily on resource availability; see the review by Liberg et al. (2000). When food resources are highly clumped and abundant as in urban or village areas, female cats form groups with densities reaching more than 2,000 individuals km^{-2}. The primary reason for group formation is to utilize and defend a large and stable food resource. In rural and nonanthropized areas, where prey items are patchily distributed and unpredictable, cats live solitarily at very low densities (<10 cats km^{-2}), and encounters among adults are rare (Kerby and Macdonald 1988).

Feline immunodeficiency virus is a worldwide-occurring pathogen of felids that induces AIDS in cats. On infection, there is a long asymptomatic carrier phase, which makes modeling FIV amenable to the simple SI (susceptibles–infecteds) structure introduced above. Previous models (e.g., Courchamp et al. 1995; Hilker et al. 2007) assumed that the number of contacts between cats is constant (giving rise to frequency-dependent transmission). While this appears reasonable in nonanthropized and suburban areas, it has been suggested that contacts of cats increase with density in rural and urban areas (Fromont et al. 1998) when home ranges tend to overlap with increasing population density. This is particularly true for dominant males and group-living females (Liberg et al. 2000). (Note that a similar argument has been made for rabies transmission in urban foxes [Smith and Harris 1991].) Feline immunodeficiency virus is transmitted by biting when males fight for monopolizing estrous females

and defend territory as well as during mating (through the bite at the neck during the mount). The number of sexual partners is higher in urban areas (as a result of the promiscuous mating system), and contacts in general are frequent in high-density areas (Natoli and De Vito 1991). This lends support for considering a density-dependent transmission rate.

In the numerical simulations presented in this article, we adopt parameter values from Courchamp et al. (1995) and Hilker et al. (2007) as follows:

$$r = 0.2,\ u = 0.1,\ d = 0.25,\ \alpha = 0.1. \tag{6}$$

Existing estimates for the frequency-dependent transmission coefficient σ_{fd} cannot be directly related to the density-dependent one, σ. As a first approximation, we utilize that the effective contact rate for density-dependent transmission is a linear function of population density. Given that Courchamp et al. (1995) estimated σ_{fd} at endemic equilibrium, we obtain $\sigma_{\mathrm{fd}} = \sigma N^*$, where N^* is the population density at endemic equilibrium. This suggests a (dimensionless) value of $\sigma = 1.5$. However, we will explore the impact of the transmission coefficient by taking it as a main bifurcation parameter.

Equilibria and Threshold Quantities: Persistence and Extinction

We show that there can be up to three endemic stationary states of model (4)–(5), plus three disease-free equilibria that always exist. We identify meaningful threshold quantities that give information about the number and location of the nontrivial stationary states. Their stability will be investigated numerically in "Bifurcation Analysis: Multistability and the (Dis-)Appearance of Oscillations."

First, let us consider the disease-free system. The Allee effect induces bistable dynamics, with the total population density approaching either the extinction state $(P_0, I_0) = (0, 0)$ or the carrying capacity $(P_2, I_2) = (1, 0)$, depending on whether the initial population density is larger or smaller than the Allee threshold u. These equilibria are separated by $(P_1, I_1) = (u, 0)$, which is always unstable.

Now, let us look for nontrivial equilibria describing endemic situations. They can be found as the intersections of the nontrivial nullclines of model (4)–(5), which are a cubic curve and a straight line, respectively. There can be either 0, 1, 2, or 3 nontrivial stationary states, as illustrated in figure 1. Detailed conditions for their existence are derived in the appendix by simple graphical phase plane analysis. Analytical solutions are too lengthy to present but can be obtained with a computer algebra system.

The effective reproductive ratio R of an infectious disease can be defined as the number of secondary infections produced by a single infected during its entire infectious period in a completely susceptible population P. In this case (see eq. [5]),

$$R = \frac{\sigma P}{\alpha + d + ru + P}. \tag{7}$$

The numerator is the number of secondary infections (σP), and the denominator is the inverse of the average infectious period that is determined by the disease-related mortality (α) and the natural mortality ($d + ru + P$). If $\sigma < 1$, R is less than unity and the disease cannot establish. Conversely, if $\sigma > 1$, the disease can be maintained in a sufficiently large population with $P > P_{\mathrm{T}}$. The critical host density P_{T} for disease establishment (henceforth referred to as disease threshold) can be determined by setting $R = 1$ and solving for

$$P_{\mathrm{T}} = \frac{\alpha + d + ru}{\sigma - 1}. \tag{8}$$

Setting $P = 1$ in equation (7), since the population will settle to its carrying capacity in the absence of disease (and being above the Allee threshold), gives the basic reproductive ratio

$$R_0 = \frac{\sigma}{\alpha + d + ru + 1}.$$

We now can summarize the number of nontrivial equilibria as in table 1 with the help of three critical values for the disease threshold P_{T}. Note that P_{T} is the point at which the linear infecteds nullcline crosses the horizontal axis (see fig. 1). The first one is associated with the carrying capacity of the host population. If $P_{\mathrm{T}} > 1$ (or, equivalently, $R_0 < 1$), density-dependent constraints prevent the population from reaching the necessary density for disease establishment. In this case, there are no nontrivial equilibria, and the system settles down to a disease-free state as described above. Table 2 shows the stabilities of the disease-free stationary states in the various threshold ranges. If $0 < P_{\mathrm{T}} < 1$ ($R_0 > 1$), the disease can persist, and the disease-free carrying capacity state (1, 0) in turn loses stability.

The second and third thresholds can be attributed solely to the Allee effect. Respectively, they are the Allee threshold u itself and

$$T_u = \frac{(u + 1)^3}{9(u^2 - u + 1)}. \tag{9}$$

We will briefly refer to T_u as the inflection threshold because beyond it the infecteds nullcline cannot intersect the

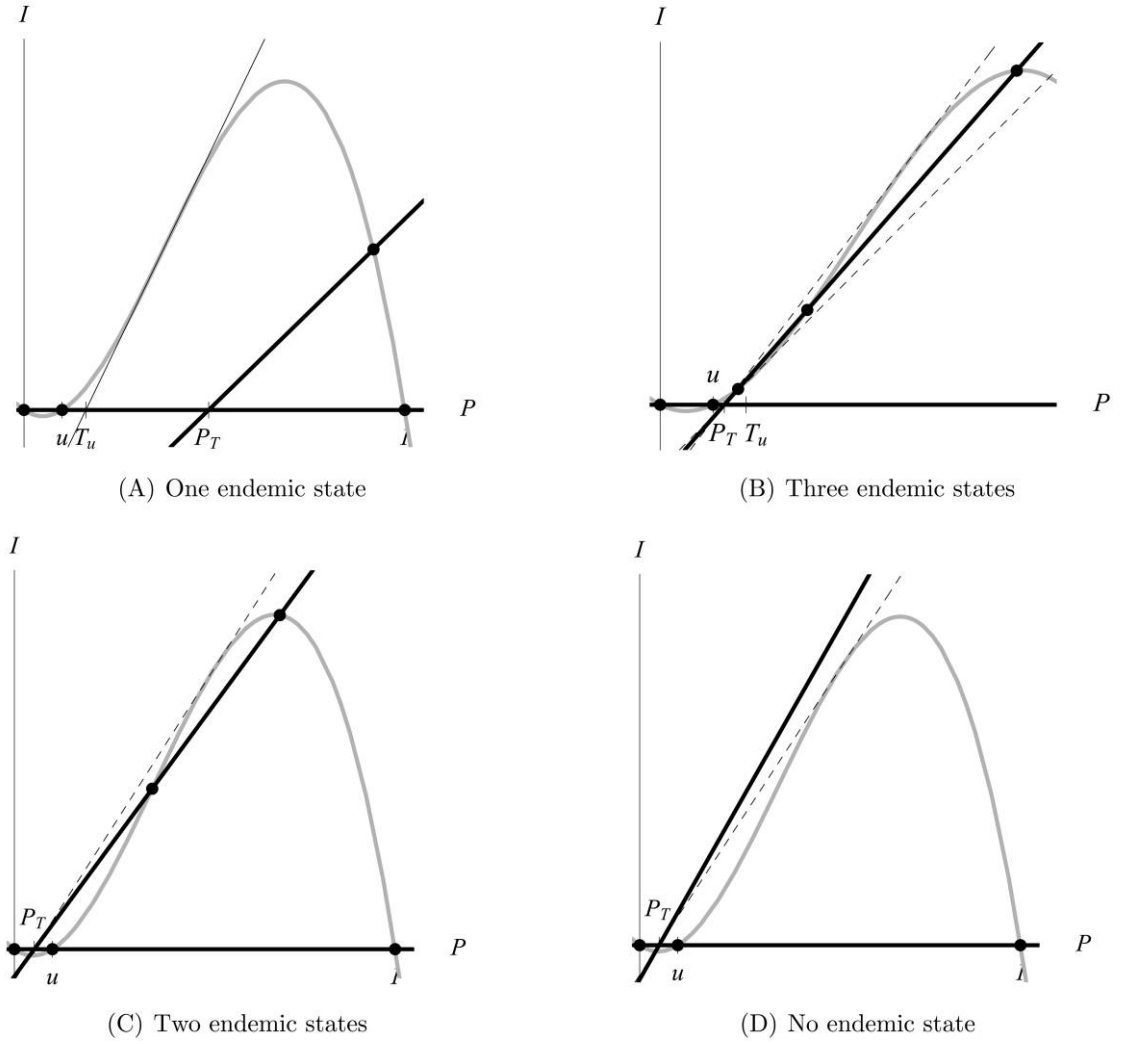

Figure 1: Graphical phase plane analysis of model (4)–(5). Stationary states (*circles*) are determined by the intersections of the nullclines of infecteds (*black line*) and total population (*gray line*). The thin line is the tangent in the cubic's inflection point crossing the horizontal axis at the inflection threshold T_u. The dashed lines are the infecteds' nullclines emanating from the disease threshold P_T that are tangent to the concave and convex branches of the cubic, respectively. Their respective slopes are s_+ and s_-. *A* shows a unique endemic equilibrium if $T_u < P_T < 1$. *B* illustrates a scenario with three endemic equilibria if $u < P_T < T_u$ and $s_- < s < s_+$. *C* and *D* indicate the occurrence of two and no endemic equilibria, respectively, depending on the slope s of the straight nullcline, if $P_T < u$.

cubic host nullcline more than once (see fig. 1*A*). Parameter T_u is the point at which the tangent line to the cubic nullcline, emanating from its inflection point, crosses the horizontal axis. Note that T_u is always larger than the Allee threshold in the parameter ranges considered (i.e., $T_u > u$ for $0 < u < 1/2$).

If the disease threshold $P_T > T_u$, there consequently is a unique endemic equilibrium (fig. 1*A*). However, for a smaller threshold density $T_u > P_T > u$, there can be up to three endemic equilibria. This depends on the slope of the infecteds' nullcline, which is given by $s := (\sigma - 1)/\sigma$ and depends solely on the transmissibility. Let s_- and s_+ be the slopes of the two dashed lines in figure 1*B*, with $s_- < s_+$. If s lies in between these two slopes, there are three endemic equilibria. If, conversely, $s < s_-$ or $s > s_+$, there is only a unique endemic equilibrium with a small or large total population density, respectively. In the case of equality, there are two endemic equilibria. The values of s_- and s_+ are defined in the appendix; they can be obtained as the respective slopes of the tangent lines to the concave and convex branches of the cubic nullcline emanating from P_T.

Table 1: Number of endemic equilibria in model (4)–(5)

	$P_T > 1$	$1 > P_T > T_u$	$T_u > P_T > u$	$u > P_T > 0$
$s > s_+$	0	1	1	0
$s_- < s < s_+$	0	1	3	2
$s < s_-$	0	1	1	2

Note: P_T, disease threshold, equation (8); T_u, inflection threshold, equation (9); u, Allee threshold; $s = (\sigma - 1)/\sigma$, slope of the infecteds' nullcline; $s_\pm$, slopes of the tangent lines to the host population's cubic nullcline (see appendix; $0 < u < 1/2$ is assumed, for which $T_u > u$).

Last, if $P_T < u$, there can be up to two endemic equilibria if $s < s_+$ (fig. 1*C*). If $s > s_+$, there is no endemic equilibrium at all (fig. 1*D*). Since the disease-free carrying capacity state $(1, 0)$ can be invaded by the disease, it is unstable, and the only attractor left is the trivial state. Hence, microparasites with a disease threshold smaller than the Allee threshold can drive their host population to extinction. This was not known in density-dependent disease transmission models before (e.g., Zhou and Hethcote 1994; de Castro and Bolker 2005). Passing the Allee threshold $P_T = u$ means that one of the endemic states—namely, the one with small population size if it existed—leaves the positive quadrant and becomes biologically unfeasible. Therefore, the number of endemic equilibria reduces from 1 to 0 or from 3 to 2 if $s > s_-$. If $s < s_-$, on the contrary, there existed only a unique endemic equilibrium with large population size for $P_T > u$, which is safe from leaving the positive quadrant. For $P_T < u$, the disease threshold is small enough to allow the establishment of an additional endemic equilibrium; that is, the number of endemic equilibria increases from 1 to 2.

The threshold $P_T < 1$ has been described by Anderson and May (1981, p. 474) for host populations with a carrying capacity. A threshold similar to $P_T < u$ has been found by Hilker et al. (2005, 2007) and Deredec and Courchamp (2006). The inflection threshold $P_T = T_u$ (as well as the occurrence of three endemic equilibria) has, to our knowledge, not been reported before. Note that T_u depends only on the Allee threshold u and is determined by the inflection point of the cubic host's nullcline. The threshold values $s_\pm$ for the slopes of the infecteds' nullcline are influenced by both demographic and epidemiological parameters (see appendix).

Bifurcation Analysis: Multistability and the (Dis-)Appearance of Oscillations

In "Equilibria and Threshold Quantities: Persistence and Extinction," we obtained information about the number of endemic equilibria and their qualitative location. Here, we investigate them quantitatively by numerical continuation and simulations, with a particular focus on their stability and cyclical behavior. As a baseline scenario, we employ the FIV parameter set (6). We already know that a necessary condition for disease spread is that transmissibility $\sigma > 1$ ("Equilibria and Threshold Quantities: Persistence and Extinction"). In what follows, we will explore the impact of the transmissibility by taking it as a main bifurcation parameter. Note that for all other parameters taken from the baseline scenario (eq. [6]), we have $s > s_+$. Later, we will also vary the virulence to allow $s_+ > s > s_-$ and $s < s_-$.

Figure 2 shows how the densities of infecteds and the total population vary with increasing transmissibility. For small values of σ ($R_0 < 1$, equivalently $P_T > 1$), the disease cannot establish ($I = 0$), and the host population either reaches the carrying capacity ($P = 1$) or becomes extinct ($P = 0$), depending on the initial condition being larger or smaller than $P = u$. This corresponds to the case $P_T > 1$ in tables 1 and 2. For $\sigma > 1.37$, the disease crosses the endemic threshold condition $R_0 = 1$ and persists. The emerging endemic equilibrium is stable, whereas the disease-free carrying capacity $(1, 0)$ becomes unstable. Figure 3*A* shows the resulting dynamics in phase plane and time plots. The total population density is depressed as a consequence of the additional disease-related mortality. The number of infecteds reaches a maximum for an intermediate transmissibility ($\sigma \approx 2.4$). Thereafter, both I and P are reduced severely. This happens when the I nullcline passes the hump of the cubic P nullcline (see fig. 3*A*).

For high values of σ, the dynamics undergo three substantial changes. First, the endemic equilibrium becomes unstable at $\sigma \approx 4.07$. Both the total population as well as the infecteds start oscillating in forms of stable limit cycles (illustrated in fig. 3*B*). Mathematically, this corresponds to a Hopf bifurcation scenario (*H* in fig. 2). The amplitudes of the oscillations are initially small but then grow quickly with increasing σ.

Second, the oscillations disappear at $\sigma \approx 4.16$. This is

Table 2: Stability of disease-free equilibria in model (4)–(5)

	$P_T > 1$	$1 > P_T > T_u$	$T_u > P_T > u$	$u > P_T > 0$
$(0, 0)$	Stable node	Stable node	Stable node	Stable node
$(u, 0)$	Saddle	Saddle	Saddle	Unstable node
$(1, 0)$	Stable node	Unstable node	Unstable node	Unstable node

Note: See table 1 for definitions.

because the increasing limit cycle collides with the equilibrium $(u, 0)$ corresponding to the Allee threshold (see fig. 3*B*, 3*C*), which is called a homoclinic bifurcation (*HL* in fig. 2). Beyond this bifurcation, the unstable endemic equilibrium still persists, but the limit cycle has disappeared. Consequently, there is no endemic attractor anymore. Since the carrying capacity state $(1, 0)$ is unstable, both the disease and the host population eventually become extinct. However, there can be a significant transient time of fluctuations before the population finally collapses (fig. 3*C*). The loss of the limit cycle also implies the loss of bistability. Note that this fundamental change occurs all of a sudden. A potentially tiny increase in σ (maybe due to random noise) might induce a catastrophic and nongradual collapse of the endemic persistence.

Third, also the unstable endemic equilibrium disappears for $\sigma > 4.7$. This occurs when the total population falls below the Allee threshold as a consequence of disease mortality. It corresponds to the case $P_T < u$, $s > s_+$ in tables 1 and 2 and is illustrated in figure 1*D*. Note that this disease-induced extinction scenario is different from the extinction dynamics after the disappearance of the limit cycle, because there are no transient fluctuations.

We now fix a different value for the virulence, $\alpha = 0.066$. In dimensional units, this corresponds to an infection length of 7.6 years rather than 5 years, as in the first part of this section. This is well within the range of 2–10 years reported for FIV (Courchamp et al. 1995). Note that with this virulence value, the slope s of the infecteds' nullcline will undergo different scenarios with increasing σ, at first $s < s_-$, then $s_- < s < s_+$, and finally $s > s_+$ (not shown here).

Figure 4*A* shows the bifurcation diagram for the infecteds; the one for the total population is qualitatively similar and therefore omitted for the sake of brevity. Again, the disease establishes in the population for $R_0 > 1$ in an initially unique endemic equilibrium. However, for higher values of σ, there appear two more bifurcations than in the previous part of this section. The first one occurs at $\sigma \approx 3.53$ when the inflection threshold $T_u > P_T$ is passed. It indicates the existence of three endemic equilibria and coincides with the transition from $s < s_-$ to $s_- < s < s_+$ (see tables 1, 2).

The two additional equilibria emerge in a saddle-node bifurcation (*SN* in fig. 4*A*). The medium branch is always unstable (the saddle point), while the lower branch initially is locally stable (the node). A portrait of the dynamics in phase plane and time is given in figure 4*B*. Note that the dynamics are tristable: depending on the starting point, the system approaches either one of the two stable endemic points or the extinction state.

The equilibrium with small population density undergoes the same changes in qualitative dynamics as the unique endemic equilibrium described in the first part. That is, it loses stability in a Hopf bifurcation at $\sigma \approx 4.03$ and gives rise to stable oscillations (fig. 4*C*). The limit cycle disappears in a homoclinic bifurcation at $\sigma \approx 4.07$. Now, the system is bistable and approaches either the endemic equilibrium with large population density or the extinction state (fig. 4*D*). However, also the remaining endemic equilibrium with large population density disappears—namely, in the second saddle-node bifurcation at $\sigma \approx 4.24$—when it coalesces with the equilibrium of medium population density. This corresponds to the transition from $s_- < s < s_+$ to $s > s_+$. From then on, the system is monostable with ultimate host population extinction (fig. 4*E*).

Two-Parameter Bifurcations: How the Dynamics Depend on the Epidemiological Setting

The results from "Bifurcation Analysis: Multistability and the (Dis-)Appearance of Oscillations" reveal that the dynamics of model (4)–(5) change profoundly not only when varying the transmissibility σ but also for different values of the virulence α. We now vary α continuously as well and study the bifurcation behavior more closely in the plane (σ, α) determined by the two epidemiological parameters.

The result is shown in figure 5. The hatched area marks the parameter region with tristable dynamics. It is delineated by solid lines describing saddle-node bifurcations and a dot-dashed line describing a homoclinic bifurcation. Tristability occurs for intermediate values of both transmissibility and virulence. In between the solid saddle-node bifurcation lines, there are three endemic equilibria. A necessary condition is $T_u > P_T > u$, but the shape of this area additionally depends on the slope s of the infecteds' nullcline and $s_\pm$ (see tables 1, 2). The dotted line marks the threshold $P_T < u$ and thus indicates that the endemic state with small population density disappears as a result of increased disease burden. Note that the classification of equilibria in tables 1 and 2 is reflected in figure 5, although

Figure 2: Bifurcation diagrams of model (4)–(5) for infecteds (*A*) and the total population (*B*). Solid lines indicate stable equilibria, dashed lines indicate unstable equilibria. Circles indicate the maximum and minimum amplitudes of limit cycle oscillations. The extinction state $(0, 0)$ is always stable and not shown here. *H* and *HL* indicate Hopf and homoclinic bifurcations, respectively. Parameter values as in equation (6).

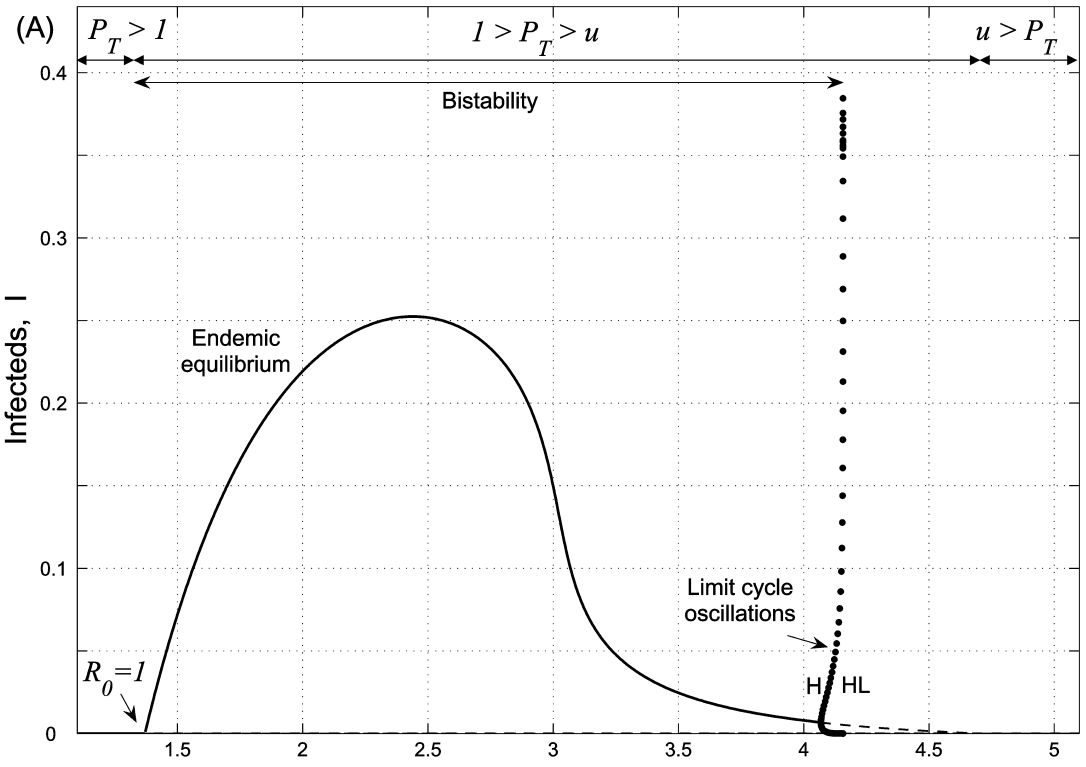
(A)
$P_T > 1$
$1 > P_T > u$
$u > P_T$
Bistability
Endemic equilibrium
Limit cycle oscillations
$R_0 = 1$
H
HL
Infecteds, I
0.4
0.3
0.2
0.1
0
1.5
2
2.5
3
3.5
4
4.5
5

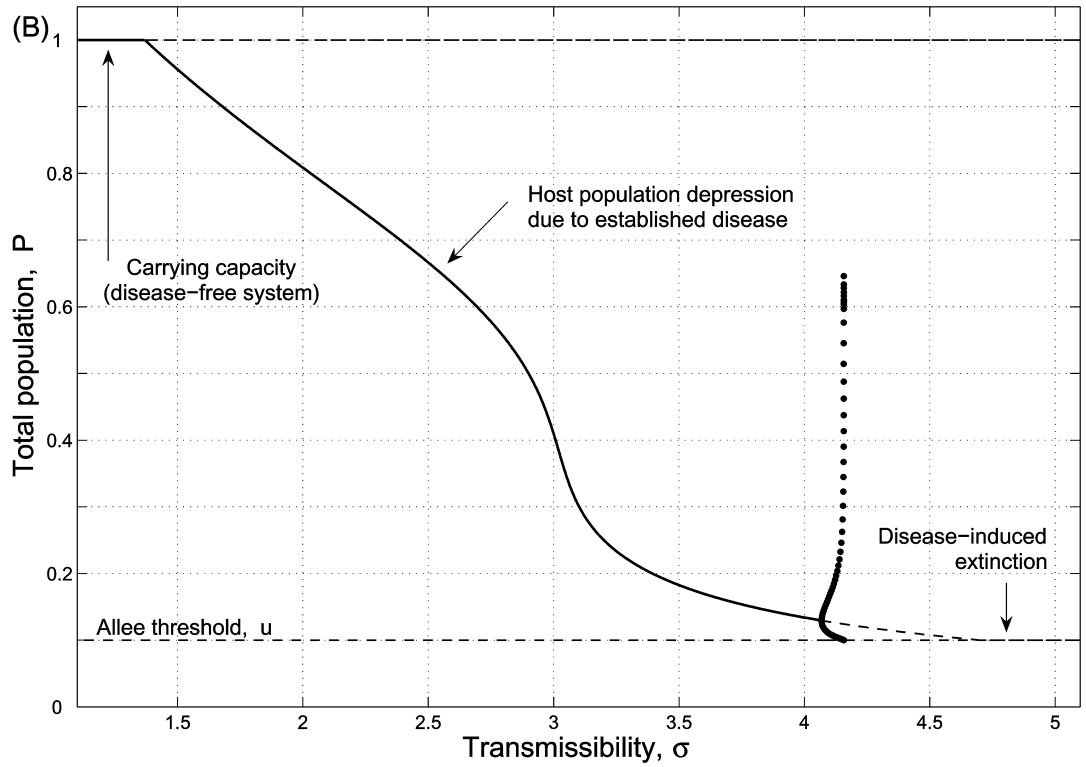
(B)
Host population depression due to established disease
Carrying capacity (disease−free system)
Disease−induced extinction
Allee threshold, u
Total population, P
Transmissibility, σ
1
0.8
0.6
0.4
0.2
0
1.5
2
2.5
3
3.5
4
4.5
5

the case $P_T > 1$ is not shown here and the division is naturally nonlinear.

Population and disease oscillate in the parameter region between the Hopf and homoclinic bifurcation (i.e., in the hatched area with decreasing stripes). Limit cycles occur in the tristable as well as the bistable region. They appear for intermediate transmissibilities and for a large enough virulence. On the right-hand side from the homoclinic bifurcation line, the periodic attractor has disappeared. The dynamics become bistable when it was tristable before or monostable when it was bistable before. Note that the monostable region corresponds to host population extinction.

The one-parameter bifurcation diagrams in figures 2 and 4*A* can be retrieved when fixing α at 0.1 and 0.066, respectively, and passing horizontally through figure 5. The stars and arrows indicate the location in parameter plane of the exemplary phase plane and time plots in previous figures.

There are two special bifurcation points. The first one is the cusp point (Kuznetsov 2004). It is located where the two saddle-node bifurcation lines meet in a cusp-shaped manner. Inside the cusp, there are three endemic states, forming a mirrored S-shape in the one-parameter bifurcation diagram in figure 4*A*. These S-shapes become more narrow toward the cusp point, where they altogether disappear and only one endemic state is left (cusp catastrophe).

The second special bifurcation point is the Bogdanov-Takens point (Kuznetsov 2004), which is located where the Hopf curve tangentially touches one of the saddle-node lines. This is also where the homoclinic curve arises. The dynamics around a Bogdanov-Takens point are highly degenerated and sensitive as a result of the saddle-node, Hopf, and homoclinic bifurcations that occur simultaneously. Moreover, this happens when the endemic state is in close proximity to the equilibrium (u, 0) corresponding to the Allee threshold (*dotted line*).

Conclusions and Discussion

The mutual impacts of a strong Allee effect and microparasites can induce rather complex population and disease transmission dynamics. The behavior observed includes sustained oscillations, multiple alternative stable stationary states, and homoclinic loops with eventual host extinction. Similar models with simpler demographics such as logistic growth do not exhibit these phenomena (e.g., Anderson and May 1991; Zhou and Hethcote 1994). They can therefore be attributed to the Allee effect. Threats by infectious diseases are pervasive for endangered species and natural as well as managed populations (Dobson and May 1986; Scott 1988; McCallum and Dobson 1995; Woodroffe 1999). The results obtained here can therefore be of significant interest, also when species reintroduction, translocation, or the biological control of pest or invasive species are considered.

Multistability, R_0*, and Control Actions*

We derived several threshold quantities for disease persistence, extinction, and the possibility of multiple stable steady states. These numbers, obtained from a simple graphical nullcline analysis, can be related to the disease threshold P_T (sometimes also referred to as critical community density). In particular, we found a new threshold T_u that can give rise to tristability and is determined solely by the Allee threshold u. Sufficient conditions for the coexistence of three endemic equilibria are $T_u > P_T > u$ and $s_+ > s > s_-$. Tristability implies that there are two endemic attractors (the third attractor is the extinction state) that correspond to different levels of disease burden, that is, number of infecteds and degree of population depression. Multiple attractors can be of great importance in areas of resource management, biological invasions, and biological control. Small perturbations of the system's state variables or parameters—for example, by noise or trends—can induce rapid and nonlinear responses, which correspond to regime shifts over short timescales (see Scheffer et al. 2001). Hence, a population in an outbreak situation with a high level of infection, for instance, could move quickly to extinction or a low infection level.

While disease control often focuses on trying to reduce the basic reproductive ratio R_0 (e.g., by vaccination or quarantine), this article suggests consideration of management measures directly perturbing the density of the total population or infecteds (e.g., selective culling). The phase plane is very "fragile" and sensitive to manipulations of the state variables. The system might readily leave its current basin of attraction and evolve to a new state (see the phase plane diagrams in figs. 3, 4). If knowledge of an emerging infectious disease or management possibilities are limited (no vaccine or treatment), removal of infected individuals appears to be one of the few remaining options (as discussed for the Tasmanian devil facial tumor disease; McCallum and Jones 2006). A widespread culling, however, needs careful monitoring, since the reduction in host population density might change the social behavior and transmission dynamics, potentially leading to negative effects, as reported for the European badger *Meles meles* in Britain, which is a reservoir for bovine tuberculosis (McDonald et al. 2008).

Management strategies need to be very carefully devised, because any action affecting the death or removal rate of infecteds (i.e., effectively α) can dramatically change the number of endemic equilibria. That is, well-intended con-

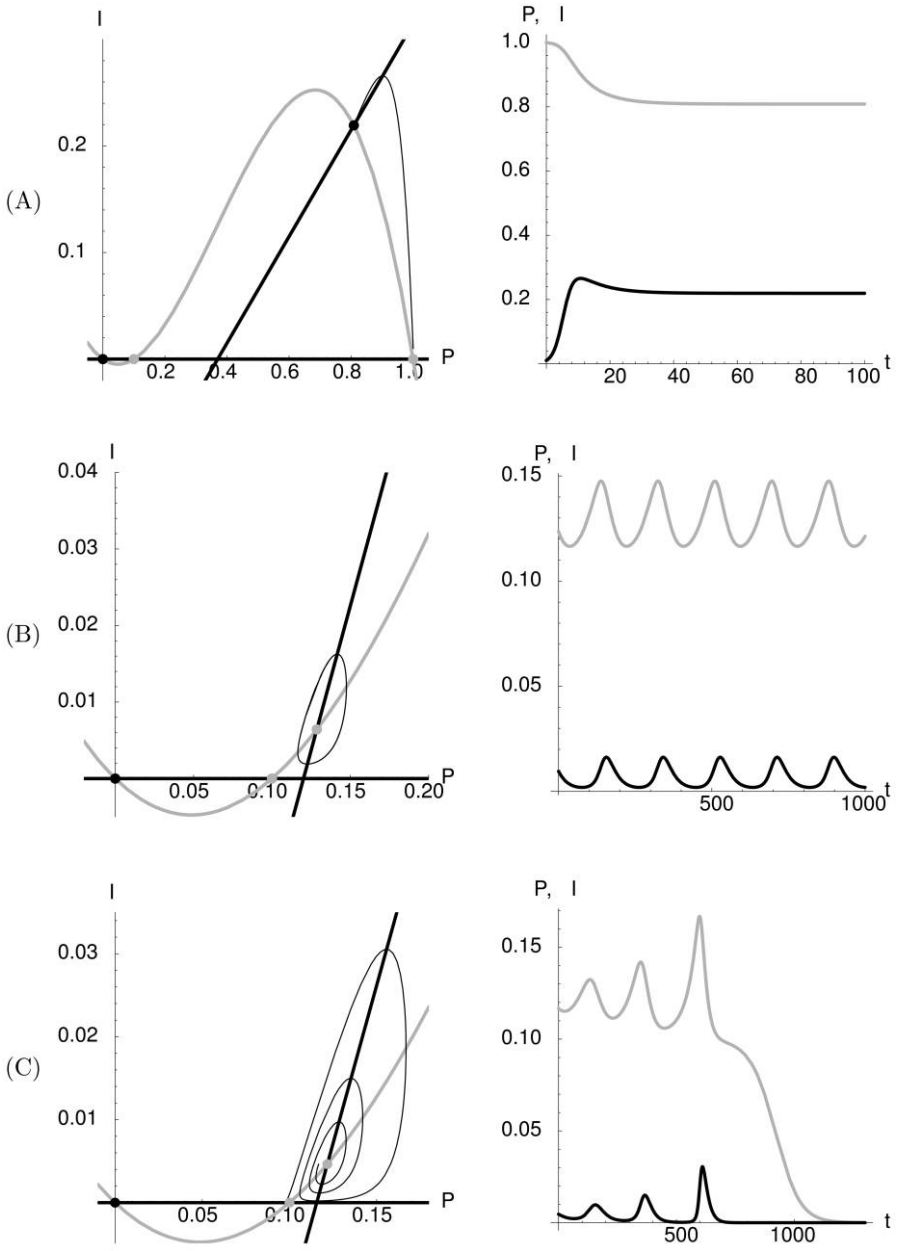

Figure 3: Phase plane diagrams (*left*) and time plots (*right*) for systems with a unique stationary state (*A*; $\sigma = 2.0$), sustained limit cycle oscillations (*B*; $\sigma = 4.08$), and an unstable endemic equilibrium after the homoclinic bifurcation, leading to the limit cycle disappearance and eventual host population extinction (*C*; $\sigma = 4.2$). Black circles indicate stable stationary states, gray circles indicate unstable stationary states. The nullclines for the total population and the infecteds are indicated by gray and black lines, respectively. Exemplary trajectories are indicated by thin lines. In the time plots (*right*), the total population is indicate by gray lines and the infecteds by black lines. Other parameters as in equation (6).

trol programs could suddenly induce the emergence of additional endemic states or the collapse of existing dynamical regimes.

Bistability in epidemic models has achieved increased interest in recent years because it has been noted that the basic reproductive ratio cannot always be used as an indicator for disease eradication anymore (e.g., Hadeler and van den Driessche 1997; Roberts 2007). In these models, the disease can persist even though R_0 has been reduced below unity ($R_0 < 1$). In our model, bi- and tristability occur for $R_0 > 1$ (see figs. 2, 4*A*). Disease control appears possible even in parameter regions far beyond $R_0 \gg 1$ (by

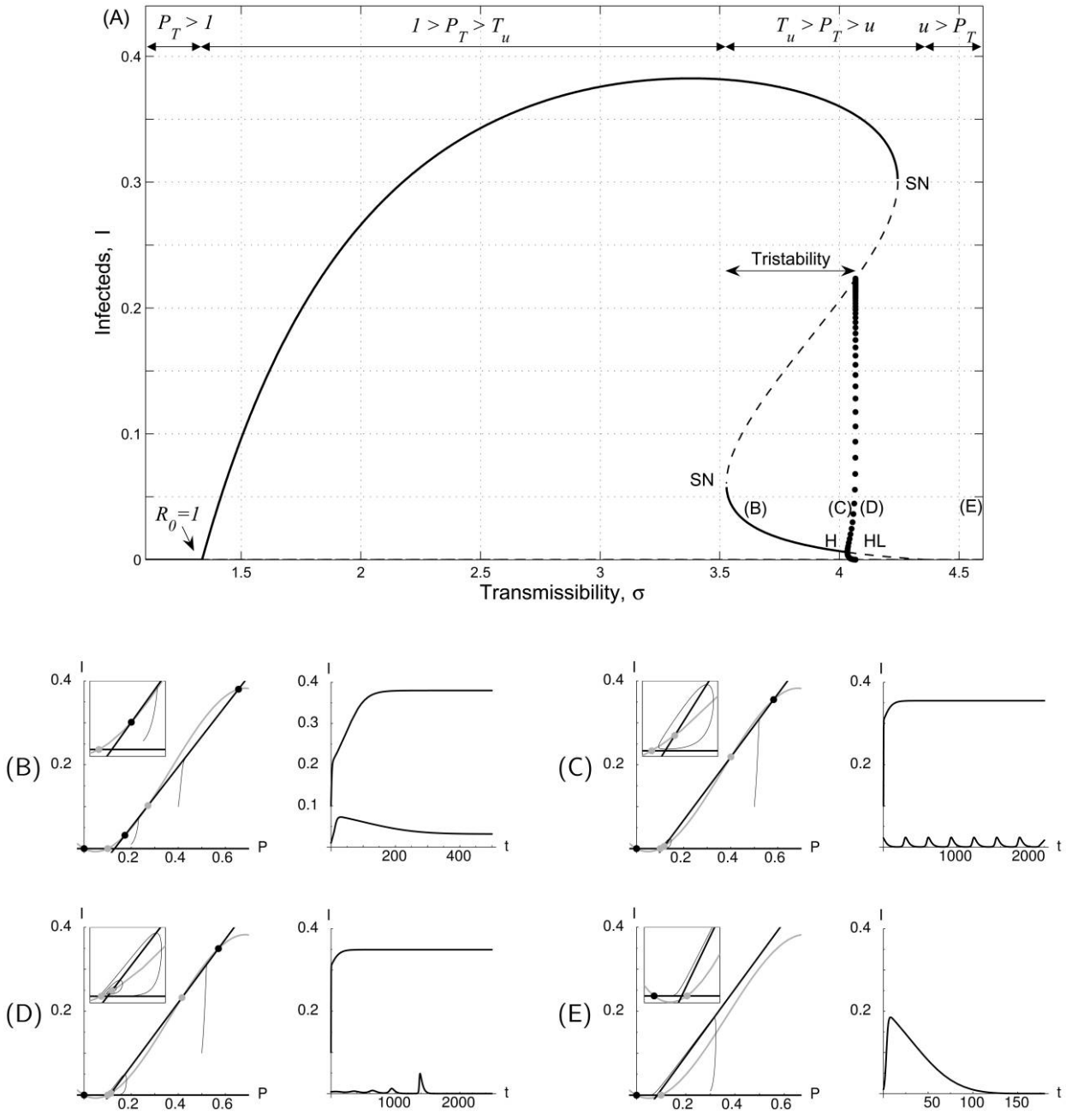

Figure 4: *A*, Bifurcation diagram of the infecteds with the virulence fixed at $\alpha = 0.066$. The extinction state $(0, 0)$ is always stable and not shown here. *SN* indicates a saddle-node bifurcation. Letters within the diagram refer to the phase plane diagrams as well as time plots in the other panels and indicate the corresponding parameter location. *B*, Tristable dynamics with three endemic equilibria, $\sigma = 3.6$. *C*, Tristable dynamics with a stable limit cycle around the endemic equilibrium with small population density, $\sigma = 4.05$. *D*, Bistable dynamics with long transients after the limit cycle disappeared in a homoclinic bifurcation, $\sigma = 4.1$. *E*, Monostable dynamics with eventual host extinction, $\sigma = 5.0$. Time plots show infecteds only for different initial conditions. Insets in the phase plane diagrams enlarge regions of interest around the Allee threshold. All other parameters as in equation (6).

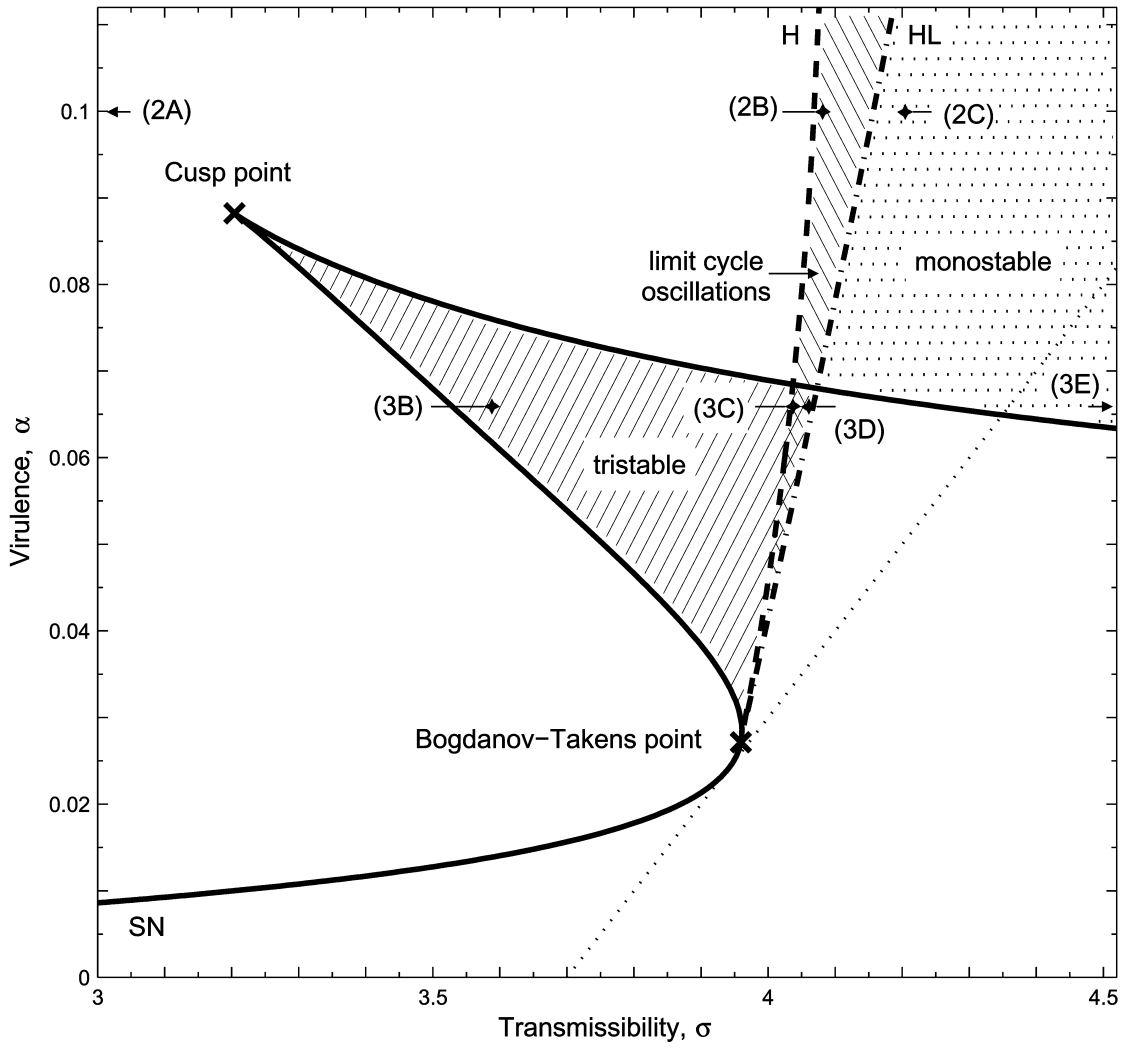

Figure 5: Two-parameter bifurcation diagram of model (4)–(5) in the disease-related parameter plane (σ, α). The dynamics can be tristable (*hatched with increasing lines*), oscillating (*hatched with decreasing lines*), monostable (*dotted*), and bistable (*white*). Solid lines correspond to saddle-node bifurcations (*SN*), dashed line to a Hopf bifurcation (*H*), and dot-dashed line to a homoclinic bifurcation (*HL*). The dotted line marks the disappearance of the endemic equilibrium with small population density. Stars and arrows refer to the location of parameters of the respective phase plane diagrams and time plots shown in corresponding previous figure panels. Other parameters as in equation (6), with $0 < u < 1/2$.

perturbations toward the low-impact state). Management actions can thus be effective in a much wider range than previously thought.

Disease Cycles

Identifying mechanisms that lead to periodic oscillations are of particular interest, since they might answer the question whether an epidemic either fades out or breaks out again. There has been a long quest for simple epidemiological models that generate oscillations (for a review, see Hethcote and Levin 1989). Some examples of the mechanisms identified are seasonal forcing (Hethcote 1973; London and Yorke 1973), a fixed period of temporary immunity (Hethcote et al. 1981), highly nonlinear incidence rates (Liu et al. 1986; Diekmann and Kretzschmar 1991), quarantine (Feng and Thieme 2000), and latency periods (Anderson et al. 1981; Swart 1989; Pugliese 1990; Roberts and Jowett 1996). We have identified a new one that induces sustained oscillations in a simple SI model and that can be traced back to the Allee effect.

The cycles in our model are generated by the interplay of disease-induced mortality, host population depensation, and density dependence in disease transmission. The os-

cillations typically occur for small population densities (see figs. 3*B*, 4*C*) when the case fatalities due to infection exceed host population growth. The shrinking population density effects a decrease in the contact rate between individuals, hence disease transmission ceases. The host population can recover, but the Allee effect induces a delay in its growth since reproduction is depressed at smaller population densities. In all this time, the number of infecteds has been decreasing and can increase again only if the population has passed the disease threshold. The same model with frequency-dependent transmission does not show sustained oscillations (Hilker et al. 2007) because disease transmission would be ongoing at small population densities, thus driving the population eventually to extinction rather than allowing it to recover and to start cycling.

The oscillation amplitudes observed in most numerical simulations are rather small. Only when the system is in a parameter regime close to the homoclinic loop, the amplitudes—as well as the cycles' period lengths—extend significantly. In this scenario, the infecteds periodically approach very small densities, so that we expect the disease to fade out as a result of stochastic effects. The host population then recovers and will be susceptible again for disease invasion if $R_0 = 1$ is passed. There is some evidence—on the basis of modeling, historic, and anecdotal information—suggesting that the Tasmanian devil experienced three cycles of catastrophic population crashes as a result of diseases and subsequent recoveries over a long timescale of 2 centuries (see Bradshaw and Brook 2005).

Disease-Induced Extinction

Density-dependent transmission was believed not to lead to host extinction, since disease transmission vanishes with disappearing population density (Anderson and May 1991; Zhou and Hethcote 1994; de Castro and Bolker 2005). However, in populations with a strong Allee effect, it is sufficient that the parasite depresses its host below a critical value (that is larger than the mere Allee threshold, since it additionally accounts for disease-related deaths). This can occur not only when the corresponding threshold $P_T < u$ is passed but also when the periodic attractor disappears as it comes too close to the Allee threshold (for large transmission coefficients and virulences, see fig. 5).

The idea of a synergetic interplay of Allee effects and disease-induced mortality in reducing host population growth was described before (Lafferty and Gerber 2002; Deredec and Courchamp 2006; Hilker et al. 2007). However, in the case of density-dependent transmission, the literature still assumes that it takes at least two alternative hosts for a parasite to drive one of its hosts to extinction (e.g., Holt and Pickering 1985). The results presented here are, to our knowledge, the first to explicitly demonstrate that host-specific parasites with density-dependent transmission and no alternative reservoir host can be fatal, too.

Bifurcation Scenario

The complex dynamical behavior observed in this model can be associated with the Bogdanov-Takens point. The existence of such a bifurcation point implies the occurrence of Hopf, homoclinic, and saddle-node bifurcations. The respective biological consequences are the following: disease cycles, population extinction with long transients, and alternatively stable states. Similar bifurcation scenarios have been observed before in some epidemic models that assumed nonlinear incidence rates (e.g., van den Driessche and Watmough 2003; Alexander and Moghadas 2004) or constant removal rates of infecteds (Wang and Ruan 2004). Van den Driessche and Watmough (2003) describe how the collapse of limit cycles in a homoclinic bifurcation can lead to a catastrophic increase in disease incidence. In our model, a homoclinic bifurcation destabilizes the attractor corresponding to small population densities. Hence, the system eventually approaches host population extinction or an endemic equilibrium with large population density (see fig. 5).

Robustness and Prospects

We would like to stress that our model is very general and based on fairly simple assumptions. It could be applied or extended to host populations and diseases with similar demographic and epidemiological structures. The numerical simulations shown in this article are based on parameter values obtained for FIV transmission dynamics among domestic cats. Estimates for σ and α (Courchamp et al. 1995) suggest a unique and stable endemic equilibrium with a prevalence of 7.2% and a host depression of 4.4%. Although this appears to be in good agreement with data (Courchamp and Pontier 1994), a more refined model for this particular disease would have to take more details into account. The main conclusion to be drawn, however, is that both population and disease dynamics might be very sensitive to parameter perturbations if a strong Allee effect would be present. The consequences could be intensified population depression, increased prevalence, cycling, or extinction.

To check the robustness of the complex dynamics, we have relaxed some model assumptions in numerical experiments to additionally account for vertical transmission and disease-reduced fertility. We could still observe limit cycle oscillations and the existence of three endemic states. The latter results from the change in convexity of the total population's nullcline at small to intermediate densities. It is thus a consequence of the function describing host

population growth. A different, noncubic form of the host growth function does not exhibit tristability (Thieme et al., forthcoming) but also leads to periodic oscillations. As discussed earlier, the inherent cycles are caused by an interplay of density-dependent disease transmission, virulence, and host growth depensation. This mechanism appears to be rather general, and we therefore expect oscillations to occur also for various other host growth functions.

The specific choice of per capita fertility rate (eq. [2]) arises from a mate shortage and crowding effects at all densities. One can, however, imagine different scenarios, for example, that fertility rates begin to decrease only under high degrees of crowding. Such a situation would make our model equations even more complicated. (Similarly, more refined disease transmission functions replacing the random mixing assumption inherent in the density-dependent form would introduce additional complexity [see Keeling 2005].) But even when the mechanistic assumptions of the present fertility rate do not hold, we expect our model to be a good phenomenological description since reproductive success is maximal at some intermediate density and then decreases with high population densities. Note that fertility function (2) corresponds to one of the simplest forms of an Allee effect (Edelstein-Keshet 1988). Parameters e and c determine the density dependence and independence, respectively, of both fertility and mortality. However, they affect only the location of the infecteds' nullcline. Complex dynamics are possible if the combination of e and c is small in relative comparison to the remaining parameters.

The inclusion of a strong Allee effect in epidemiological models induces dynamics that are much more complicated than previously thought. Endogenously induced periodic oscillations are possible as well as the simultaneous coexistence of multiple endemic equilibria. For large transmissibilities and/or large virulences, the most likely consequence of the synergetic interplay between infectious diseases and Allee effects is population extinction. Probably as a result of historic reasons, Allee effects have been largely neglected in epidemiological modeling. However, they are to be expected for many animal and plant species (Berec et al. 2007; Courchamp et al. 2008; Molnár et al. 2008). The qualitative conclusions from this article can therefore be helpful in assessing the impact of parasites in populations subject to a strong Allee effects.

Acknowledgments

F.M.H. acknowledges R. Casagrandi and S. V. Petrovskii for useful hints during an earlier stage of this work; P. K. Molnár, H. R. Thieme, and P. van den Driessche for comments on the manuscript; and support from an Alberta Ingenuity and Honorary Killam postdoctoral fellowship. We are grateful to two anonymous reviewers for their suggestions that helped to improve this article.

APPENDIX

Existence of Endemic Equilibria: Phase Plane Analysis

We investigate the number of nontrivial stationary states (endemic equilibria) and derive the conditions for their existence. This will give us the threshold quantities identified in "Equilibria and Threshold Quantities: Persistence and Extinction." Our strategy is based solely on simple graphical phase plane analysis making use of the nullclines (zero-growth isoclines).

Endemic equilibria of model (4)–(5) are determined by the intersections of the nontrivial nullclines of the total population P and infecteds I. Respectively, they are given by

$$I(P) = \frac{r}{\alpha}P(1-P)(P-u) =: n_P(P),$$

$$I(P) = \frac{-\alpha - d - ru}{\sigma} + \frac{\sigma - 1}{\sigma}P =: n_I(P).$$

Note that n_P is a cubic polynomial in P and n_I is a straight line. The slope $s := (\sigma - 1)/\sigma$ of the straight line is determined only by the transmissibility. If $\sigma < 1$, the nullcline is decreasing, and there will be no intersection with n_P in the positive quadrant. We henceforth assume $\sigma > 1$.

In what follows, we first fix the root P_T of the straight line—that is, the intersection with the horizontal axis—and then vary its slope to consider the number and location of intersections (endemic equilibria). Illustrations are shown in figure 1. The root P_T is the disease threshold, as given in equation (8). It is positive for $\sigma > 1$. We can now distinguish the following four cases of the relative locations of P_T, the Allee threshold u, the carrying capacity 1, and the inflection threshold T_u. The latter is the root of the tangent line through the cubic's inflection point and can be computed as in equation (9). We still assume $0 < u < 1/2$ (i.e., $T_u > u$). When $1/2 < u < 1$ (i.e., $T_u < u$), a similar analysis yields at most two nontrivial stationary states.

First, consider $P_T < u$. Exemplary nullclines are sketched in figure 1*C* and 1*D*. If the slope s of n_I is smaller (larger) than the slope s_+ of the tangent line to the cubic n_P with the same root P_T, then there will be two (0) endemic equilibria in the positive quadrant (see fig. 1*C*, 1*D*). The aforementioned tangent line with root ($P = P_T$, $I = 0$) and slope $s_+ := n_P'(P_+)$ is defined by

$$t(P_T) = n_P(P_+) + n'_P(P_+)(P_T - P_+) = 0,$$

where P_+ is implicitly given as a root of this cubic equation and

$$n'_P(P) = \frac{r}{\alpha}[-3P^2 + 2(1 + u)P - u].$$

Comparing s_+ with the slope s of the straight nullcline, we obtain the following: there is a unique endemic equilibrium if $s = s_+$, no endemic equilibrium if $s > s_+$, and two endemic equilibria if $s < s_+$.

Second, consider $u < P_T < T_u$, as sketched in figure 1*B*. The straight nullcline can now be tangent to the cubic nullcline n_P at two different locations in the positive quadrant: at $P = P_+$ to the concave branch with slope $s_+ := n'_P(P_+)$ and at $P = P_-$ to the convex branch with slope $s_- := n'_P(P_-)$. Comparing the slope of n_I with the slopes of these two tangential lines, we obtain the following: there is (1) a unique endemic equilibrium (P_3^*, I_3^*), with $P_T < P_3^* < T_u$ if $s > s_+$; (2) three endemic equilibria $(P^*_{3,4,5}, I^*_{3,4,5})$, with $P_T < P_3^* < T_u$, $P_- < P_4^* < P_+$, and $T_u < P_5^* < 1$ if $s_- < s < s_+$; (3) a unique endemic equilibrium (P_5^*, I_5^*), with $T_u < P_5^* < 1$ if $s < s_-$; and (4) two endemic equilibria if $s = s_-$ or $s = s_+$, with one of them being a saddle node.

Third, consider $T_u < P_T < 1$, as in figure 1*A*. Then there is always a unique endemic equilibrium (P^*, I^*), with $P_T < P^* < 1$, independent of the slope s.

Fourth and last, consider $P_T > 1$. Then there is no intersection of n_I and n_P in the positive quadrant. Hence, endemic equilibria do not exist.

Literature Cited

Alexander, M. E., and S. M. Moghadas. 2004. Periodicity in an epidemic model with a generalized non-linear incidence. Mathematical Biosciences 189:75–96.

Allee, W. C. 1938. The social life of animals. Norton, New York.

Altizer, S., C. L. Nunn, P. H. Thrall, J. L. Gittleman, J. Antonovics, A. A. Cunningham, A. P. Dobson, et al. 2003. Social organization and parasite risk in mammals: integrating theory and empirical studies. Annual Review of Ecology, Evolution, and Systematics 34: 517–547.

Amarasekare, P. 1998. Allee effects in metapopulation dynamics. American Naturalist 152:298–302.

Anderson, R. M., and R. M. May. 1979. Population biology of infectious diseases. I. Nature 280:361–367.

———. 1981. The population dynamics of microparasites and their invertebrate hosts. Philosophical Transactions of the Royal Society B: Biological Sciences 291:451–524.

———. 1991. Infectious diseases of humans: dynamics and control. Oxford University Press, Oxford.

Anderson, R. M., H. C. Jackson, R. M. May, and A. M. Smith. 1981. Population dynamics of fox rabies in Europe. Nature 289:765–770.

Angulo, E., G. W. Roemer, L. Berec, J. Gascoigne, and F. Courchamp. 2007. Double Allee effects and extinction in the island fox. Conservation Biology 21:1082–1091.

Bailey, N. T. J. 1975. The mathematical theory of infectious diseases and its applications. 2nd ed. Charles Griffin, London.

Berec, L., E. Angulo, and F. Courchamp. 2007. Multiple Allee effects and population management. Trends in Ecology & Evolution 22: 185–191.

Boukal, D. S., and L. Berec. 2002. Single-species models of the Allee effect: extinction boundaries, sex ratios and mate encounters. Journal of Theoretical Biology 218:375–394.

Bradshaw, C. J. A., and B. W. Brook. 2005. Disease and the devil: density-dependent epidemiological processes explain historical population fluctuations in the Tasmanian devil. Ecography 28:181–190.

Burrows, R., H. Hofer, and M. L. East. 1995. Population dynamics, intervention and survival in African wild dogs (*Lycaon pictus*). Proceedings of the Royal Society B: Biological Sciences 262:235–245.

Christe, P., S. Morand, and J. Michaux. 2006. Biological conservation and parasitism. Pages 593–613 *in* S. Morand, B. R. Krasnov, and R. Poulin, eds. Micromammals and macroparasites. Springer, Tokyo.

Cleaveland, S., T. Mlengeya, M. Kaare, D. Haydon, T. Lembo, M. K. Laurenson, and C. Packer. 2007. The conservation relevance of epidemiological research into carnivore viral diseases in the Serengeti. Conservation Biology 21:612–622.

Clifford, D. L., J. A. K. Mazet, E. J. Dubovi, D. K. Garcelon, T. J. Coonan, P. A. Conrad, and L. Munson. 2006. Pathogen exposure in endangered island fox (*Urocyon littoralis*) populations: implications for conservation management. Biological Conservation 131:230–243.

Courchamp, F., and P. Pontier. 1994. Feline immunodeficiency virus: an epidemiological review. Comptes Rendus de l'Academie des Sciences Serie III Sciences de la Vie 317:1123–1134.

Courchamp, F., D. Pontier, M. Langlais, and M. Artois. 1995. Population dynamics of feline immunodeficiency virus within cat populations. Journal of Theoretical Biology 175:553–560.

Courchamp, F., T. Clutton-Brock, and B. Grenfell. 1999. Inverse density dependence and the Allee effect. Trends in Ecology & Evolution 14:405–410.

———. 2000. Multipack dynamics and the Allee effect in the African wild dog, *Lycaon pictus*. Animal Conservation 3:277–285.

Courchamp, F., L. Berec, and J. Gascoigne. 2008. Allee effects in ecology and conservation. Oxford University Press, New York.

Daszak, P., L. Berger, A. A. Cunningham, A. D. Hyatt, D. E. Green, and R. Speare. 1999. Emerging infectious diseases and amphibian population declines. Emerging Infectious Diseases 5:735–748.

de Castro, F., and B. Bolker. 2005. Mechanisms of disease-induced extinction. Ecology Letters 8:117–126.

Dennis, B. 1989. Allee effects: population growth, critical density, and the chance of extinction. Natural Resource Modeling 3:481–538.

Deredec, A., and F. Courchamp. 2006. Combined impacts of Allee effects and parasitism. Oikos 112:667–679.

Diekmann, O., and J. A. P. Heesterbeek. 2000. Mathematical epidemiology of infectious diseases: model building, analysis and interpretation. Wiley, New York.

Diekmann, O., and M. Kretzschmar. 1991. Patterns in the effects of infectious diseases on population growth. Journal of Mathematical Biology 29:539–570.

Dobson, A. P., and R. M. May. 1986. Disease and conservation. Pages 345–365 *in* M. E. Soulé, ed. Conservation biology. Sinauer, Sunderland, MA.

Dobson, A. P., and J. Poole. 1998. Conspecific aggregation and conservation biology. Pages 193–208 *in* T. M. Caro, ed. Behavioral ecology and conservation biology. Oxford University Press, Oxford.

Edelstein-Keshet, L. 1988. Mathematical models in biology. McGraw-Hill, New York.

Feng, Z., and H. R. Thieme. 2000. Endemic models with arbitrarily distributed periods of infection. II. Fast disease dynamics and permanent recovery. SIAM Journal on Applied Mathematics 61:983–1012.

Fromont, E., D. Pontier, and M. Langlais. 1998. Dynamics of a feline retrovirus (FeLV) in host populations with variable spatial structure. Proceedings of the Royal Society B: Biological Sciences 265: 1097–1104.

Gerber, L. R., H. McCallum, K. D. Lafferty, J. L. Sabo, and A. Dobson. 2005. Exposing extinction risk analysis to pathogens: is disease just another form of density dependence? Ecological Applications 15: 1402–1414.

Gruntfest, Y., R. Arditi, and Y. Dombrovsky. 1997. A fragmented population in a varying environment. Journal of Theoretical Biology 185:539–547.

Hadeler, K. P., and P. van den Driessche. 1997. Backward bifurcation in epidemic control. Mathematical Biosciences 146:15–35.

Harvell, C. D., C. E. Mitchell, J. R. Ward, S. Altizer, A. P. Dobson, R. S. Ostfeld, and M. D. Samuel. 2002. Climate warming and disease risks for terrestrial and marine biota. Science 296:2158–2162.

Haydon, D. T., M. K. Laurenson, and C. Sillero-Zubiri. 2002. Integrating epidemiology into population viability analysis: managing the risk posed by rabies and canine distemper to the Ethiopian wolf. Conservation Biology 16:1372–1385.

Hethcote, H. W. 1973. Asymptotic behavior in a deterministic epidemic model. Bulletin of Mathematical Biology 35:607–614.

Hethcote, H. W., and S. A. Levin. 1989. Periodicity in epidemiological models. Pages 193–211 *in* S. A. Levin, T. G. Hallam, and L. J. Gross, eds. Applied mathematical ecology. Springer, New York.

Hethcote, H. W., H. W. Stech, and P. van den Driessche. 1981. Nonlinear oscillations in epidemic models. SIAM Journal on Applied Mathematics 40:1–9.

Hilker, F. M., M. A. Lewis, H. Seno, M. Langlais, and H. Malchow. 2005. Pathogens can slow down or reverse invasion fronts of their hosts. Biological Invasions 7:817–832.

Hilker, F. M., M. Langlais, S. V. Petrovskii, and H. Malchow. 2007. A diffusive SI model with Allee effect and application to FIV. Mathematical Biosciences 206:61–80.

Holt, R. D., and J. Pickering. 1985. Infectious disease and species coexistence: a model of Lotka-Volterra form. American Naturalist 126:196–211.

Hopf, F. A., and F. W. Hopf. 1985. The role of the Allee effect in species packing. Theoretical Population Biology 27:27–50.

Hudson, P. J., A. Rizzoli, B. T. Grenfell, H. Heesterbeek, and A. P. Dobson. 2001. The ecology of wildlife diseases. Oxford University Press, Oxford.

Keeling, M. J. 2005. Extensions to mass-action mixing. Pages 107–142 *in* K. Cuddington and B. E. Beisner, eds. Ecological paradigms lost: routes of theory change. Elsevier, Burlington, MA.

Kerby, G., and D. W. Macdonald. 1988. Cat society and the consequence of colony size. Pages 67–81 *in* D. C. Turner and P. Bateson, eds. The domestic cat: the biology of its behaviour. 1st ed. Cambridge University Press, Cambridge.

Kuznetsov, Y. A. 2004. Elements of applied bifurcation theory. Springer, New York.

Lafferty, K. D., and L. R. Gerber. 2002. Good medicine for conservation biology: the intersection of epidemiology and conservation theory. Conservation Biology 16:593–604.

Lewis, M. A., and P. Kareiva. 1993. Allee dynamics and the spread of invading organisms. Theoretical Population Biology 43:141–158.

Liberg, O., M. Sandell, D. Pontier, and E. Natoli. 2000. Density, spatial organisation and reproductive tactics in the domestic cat and other felids. Pages 119–147 *in* D. C. Turner and P. Bateson, eds. The domestic cat: the biology of its behaviour. 2nd ed. Cambridge University Press, Cambridge.

Liu, W., S. A. Levin, and Y. Iwasa. 1986. Influence of non-linear incidence rates upon the behaviour of SIRS epidemiological models. Journal of Mathematical Biology 23:187–204.

London, W. P., and J. A. Yorke. 1973. Recurrent outbreaks of measles, chickenpox and mumps. I. Seasonal variation in contact rates. American Journal of Epidemiology 98:453–468.

McCallum, H., and A. Dobson. 1995. Detecting disease and parasite threats to endangered species and ecosystems. Trends in Ecology & Evolution 10:190–194.

McCallum, H., and M. Jones. 2006. To lose both would look like carelessness: Tasmanian devil facial tumour disease. PLoS Biology 4:1671–1674.

McCallum, H., N. Barlow, and J. Hone. 2001. How should pathogen transmission be modelled? Trends in Ecology & Evolution 16:295–300.

McDonald, R. A., R. J. Delahay, S. P. Carter, G. C. Smith, and C. L. Cheeseman. 2008. Perturbing implications of wildlife ecology for disease control. Trends in Ecology & Evolution 23:53–56.

Møller, A. P., R. Dufva, and K. Allander. 1993. Parasites and the evolution of host social behavior. Advances in the Study of Behavior 22:65–102.

Molnár, P. K., A. E. Derocher, M. A. Lewis, and M. K. Taylor. 2008. Modelling the mating system of polar bears: a mechanistic approach to the Allee effect. Proceedings of the Royal Society B: Biological Sciences 275:217–226.

Natoli, E., and E. De Vito. 1991. Agonistic behaviour, dominance rank and copulatory success in a large multi-male feral cat, *Felis catus* L., colony in central Rome. Animal Behaviour 42:227–241.

Petrovskii, S. V., H. Malchow, F. M. Hilker, and E. Venturino. 2005. Patterns of patchy spread in deterministic and stochastic models of biological invasion and biological control. Biological Invasions 7:771–793.

Pugliese, A. 1990. Population models for diseases with no recovery. Journal of Mathematical Biology 28:65–82.

Roberts, M. G. 2007. The pluses and minuses of R_0. Journal of the Royal Society Interface 4:949–961.

Roberts, M. G., and J. Jowett. 1996. An SEI model with density-dependent demographics and epidemiology. IMA Journal of Mathematics Applied in Medicine and Biology 13:245–257.

Scheffer, M., S. Carpenter, J. A. Foley, C. Folke, and B. Walker. 2001. Catastrophic shifts in ecosystems. Nature 413:591–596.

Scott, M. E. 1988. The impact of infection and disease on animal populations: implications for conservation biology. Conservation Biology 2:40–56.

Smith, G. C., and S. Harris. 1991. Rabies in urban foxes (*Vulpes vulpes*) in Britain: the use of a spatial stochastic simulation model to examine the pattern of spread and evaluate the efficacy of different control régimes. Philosophical Transactions of the Royal Society B: Biological Sciences 334:459–479.

Smith, K. F., D. F. Sax, and K. D. Lafferty. 2006. Evidence for the role of infectious disease in species extinction and endangerment. Conservation Biology 20:1349–1357.

Stephens, P. A., and W. J. Sutherland. 1999. Consequences of the Allee effect for behaviour, ecology and conservation. Trends in Ecology & Evolution 14:401–405.

Stephens, P. A., W. J. Sutherland, and R. P. Freckleton. 1999. What is the Allee effect? Oikos 87:185–190.

Swart, J. H. 1989. Hopf bifurcation and stable limit cycle behavior in the spread of infectious disease, with special application to fox rabies. Mathematical Biosciences 95:199–207.

Thieme, H. R., T. Dhirasakdanon, Z. Han, and R. Trevino. Forthcoming. Species decline and extinction: synergy of infectious diseases and (Allee) effect? Journal of Biological Dynamics.

van den Driessche, P., and J. Watmough. 2003. Epidemic solutions and endemic catastrophes. Pages 247–257 *in* S. Ruan, G. S. K. Wolkowicz, and J. Wu, eds. Dynamical systems and their applications in biology. American Mathematical Society, Providence, RI.

Volterra, V. 1938. Population growth, equilibria, and extinction under specified breeding conditions: a development and extension of the logistic curve. Human Biology 10:3–11.

Wang, G., X.-G. Liang, and F.-Z. Wang. 1999. The competitive dynamics of populations subject to an Allee effect. Ecological Modelling 124:183–192.

Wang, W., and S. Ruan. 2004. Bifurcations in an epidemic model with constant removal rate of the infectives. Journal of Mathematical Analysis and Applications 291:775–793.

Woodroffe, R. 1999. Managing disease threats to wild mammals. Animal Conservation 2:185–193.

Zhou, J., and H. W. Hethcote. 1994. Population size dependent incidence in models for diseases without immunity. Journal of Mathematical Biology 32:809–834.

Associate Editor: Matthew Keeling
Editor: Donald L. DeAngelis